processes

MDPI

Review

Numerical Modeling of Ammonia-Fueled Protonic-Ion Conducting Electrolyte-Supported Solid Oxide Fuel Cell (H-SOFC): A Brief Review

Md. Mosfiqur Rahman [1,2,*], Abdalla M. Abdalla [3], Lukman Ahmed Omeiza [1], Veena Raj [1], Shammya Afroze [4], Md. Sumon Reza [5], Mahendra Rao Somalu [6] and Abul K. Azad [1,*]

1 Faculty of Integrated Technologies, Universiti Brunei Darussalam, Gadong BE1410, Brunei; 21h8401@ubd.edu.bn (L.A.O.); veena.raj@ubd.edu.bn (V.R.)
2 Faculty of Science & Information Technology, Daffodil International University, Dhaka 1341, Bangladesh
3 Mechanical Engineering Department, Faculty of Engineering, Suez Canal University, Ismailia 41522, Egypt; abdalla.m.a1984@gmail.com
4 Faculty of Physics and Technical Sciences, L.N. Gumilyov Eurasian National University, Astana 010008, Kazakhstan; afroze_sh@enu.kz
5 Research Institute of New Chemical Technologies, Faculty of Natural Sciences, L.N. Gumilyov Eurasian National University, Astana 010008, Kazakhstan; reza_m@enu.kz
6 Fuel Cell Institute, Universiti Kebangsaan Malaysia, Bangi 43600, Malaysia; mahen@ukm.edu.my
* Correspondence: mosfiqurju35@gmail.com (M.M.R.); abul.azad@ubd.edu.bn (A.K.A.)

Abstract: Solid oxide fuel cells with protonic ion conducting electrolytes (H-SOFCs) are recognized and anticipated as eco-friendly electrochemical devices fueled with several kinds of fuels. One distinct feature of SOFCs that makes them different from others is fuel flexibility. Ammonia is a colorless gas with a compound of nitrogen and hydrogen with a distinct strong smell at room temperature. It is easily dissolved in water and is a great absorbent. Ammonia plays a vital role as a caustic for its alkaline characteristics. Nowadays, ammonia is being used as a hydrogen carrier because it has carbon-free molecules and prosperous physical properties with transportation characteristics, distribution options, and storage capacity. Using ammonia as a fuel in H-SOFCs has the advantage of its ammonia cracking attributes and quality of being easily separated from generated steam. Moreover, toxic NO_x gases are not formed in the anode while using ammonia as fuel in H-SOFCs. Recently, various numerical studies have been performed to comprehend the electrochemical and physical phenomena of H-SOFCs in order to develop a feasible and optimized design under different operating conditions rather than doing costlier experimentation. The aim of this concisely reviewed article is to present the current status of ammonia-fueled H-SOFC numerical modeling and the application of numerical modeling in ammonia-fueled H-SOFC geometrical shape optimization, which is still more desirable than traditional SOFCs.

Keywords: numerical modeling; fuel cells; solid oxide fuel cell; ammonia-fueled solid oxide fuel cell; protonic conducting fuel cells; physical phenomena; design analysis

Citation: Rahman, M.M.; Abdalla, A.M.; Omeiza, L.A.; Raj, V.; Afroze, S.; Reza, M.S.; Somalu, M.R.; Azad, A.K. Numerical Modeling of Ammonia-Fueled Protonic-Ion Conducting Electrolyte-Supported Solid Oxide Fuel Cell (H-SOFC): A Brief Review. *Processes* **2023**, *11*, 2728. https://doi.org/10.3390/pr11092728

Academic Editors: Zucheng Wu and Prashant K. Sarswat

Received: 7 July 2023
Revised: 20 August 2023
Accepted: 11 September 2023
Published: 12 September 2023

1. Introduction

Numerous factors, including the world's rapidly rising energy needs, public concern for environmental security and safety, and rising fossil fuel prices, have led individuals to seek alternative or renewable energy sources. Fossil fuel resources are extremely finite and are expected to run out early in the twenty-first century. If a sustainable and environmentally benign resource is not made available soon, the global demand for fossil fuels will persistently increase, leading to an energy availability crisis [1,2]. Small power production technologies like fuel cells, micro-turbines, and wind turbines can be crucial to satisfying consumer demand for green energy [3–5]. Since they combine heat and power systems, fuel cells have attracted more attention than any other small-scale power generation system.

Fuel cells enable homeowners to produce some of the electricity they require, lowering the amount of electricity that is purchased from power-producing companies [6,7].

The static energy conversion technology known as fuel cells produces water as a byproduct while converting the chemical energy of fuel into electrical energy. Figure 1 shows the chart of different kinds of fuel cells.

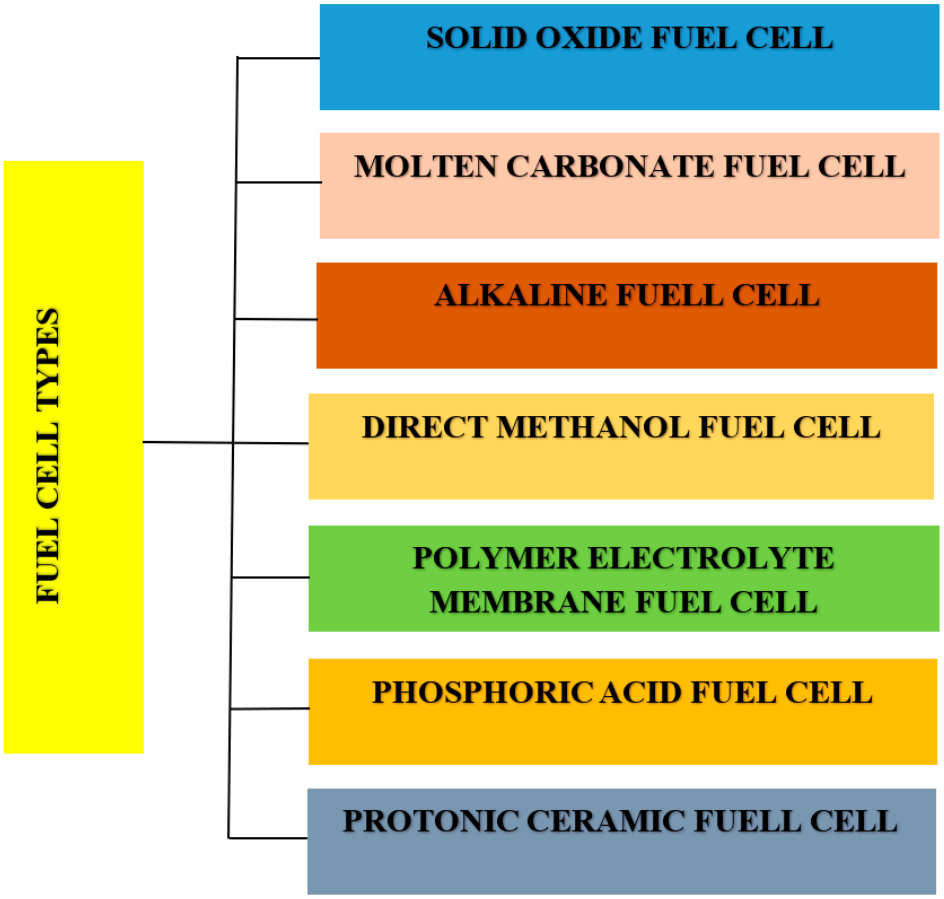

Figure 1. Different types (most common) of fuel cells.

With the development of power conversion devices, more and more research is being conducted on solid oxide fuel cells in order to lower their high temperature and high installation costs, enhance their cell performance at intermediate temperatures, and so on. One of the most cutting-edge designs for medium and large-scale applications, solid oxide fuel cells come in a variety of geometric configurations, including planar, tubular, flat-tubular, and micro-tubular.

The main challenge of this research field is to provide a lesser or zero carbon-containing fuel supply to the SOFC that would pollute the environment in a small percentage. Regarding this, ammonia might be the ideal fuel for SOFCs due to its attributes as green and carbon-neutral fuel characteristics and the fact that it contains hydrogen in its bond, which makes ammonia more user-friendly than hydrogen [8,9]. It also offers significant storage capacity, good transmission qualities, and a high volumetric energy density. Additionally, it decomposes into free nitrogen and hydrogen [2,10–13].

But, ammonia-fueled SOFCs face unique challenges as an emerging technology that requires a deeper understanding of their complex electrochemical and transport phenomena. For example, ammonia adsorption, ammonia decomposition, transport of ions, and species inside the cell are still complex phenomena to understand. Numerous efforts have been made using a variety of technologies to comprehend the connection between the performance of ammonia-fueled SOFCs and their operating conditions. Numerical models can simulate and study these complex processes, providing an extended insight into

the fundamental mechanisms governing cell performance. Through parametric studies, sensitivity analyses, and optimization techniques, numerical modeling helps to identify the optimal configurations that lead to enhanced cell performance and efficiency. The kinetics of ammonia decomposition are critical to the efficient usage of ammonia as a fuel. Numerical modeling can clarify the rate-limiting steps and the impact of various factors on the decomposition process, providing guidance for reactor design and catalyst selection. Numerical modeling helps in studying the species and thermal transport phenomena, leading to a better understanding and optimization of the transport processes. Ammonia-fueled SOFCs are subject to diverse degradation mechanisms that can impact long-term stability. Numerical models can simulate these degradation processes, enabling researchers to develop strategies to mitigate them and improve cell durability.

The integration of ammonia as a fuel in SOFCs has opened up new possibilities. The main objective of this review article is to critically understand the application of ammonia in proton-conducting electrolyte-supported SOFCs to predict the performance of SOFCs under different operating conditions. Many research studies have been performed on the numerical modeling of SOFCs, but very few have been performed on ammonia-fueled H-SOFCs, especially at intermediate temperatures. We have discussed and analyzed the role of numerical models for ammonia-fueled H-SOFCs. This attempt will make it easier for researchers to comprehend the mathematical methods for future ammonia-fueled H-SOFC improvements. Finally, recommendations have been made for the future trajectory of numerical modeling in the field of H-SOFCs.

2. General Principle and Working Nature of Ammonia-Fueled H-SOFC

A solid oxide fuel cell (SOFC) is an electrochemical conversion device that generates energy by directly oxidizing a fuel. Fuel cells are normally characterized by their electrolyte material; the SOFC uses hard ceramic electrolytes and operates at temperatures up to 1000 °C [14,15]. A schematic representation of the working principle of NH_3-fueled H-SOFCs is illustrated in Figure 2. The SOFC consists of an anode, cathode, electrolyte, and interconnector. Hydrogen is oxidized on the anode side, and oxygen reduction occurs on the cathode side. When hydrogen oxidizes, it produces protons (H^+) and electrons, which are transported through the electrolyte and external circuit to the cathode chamber.

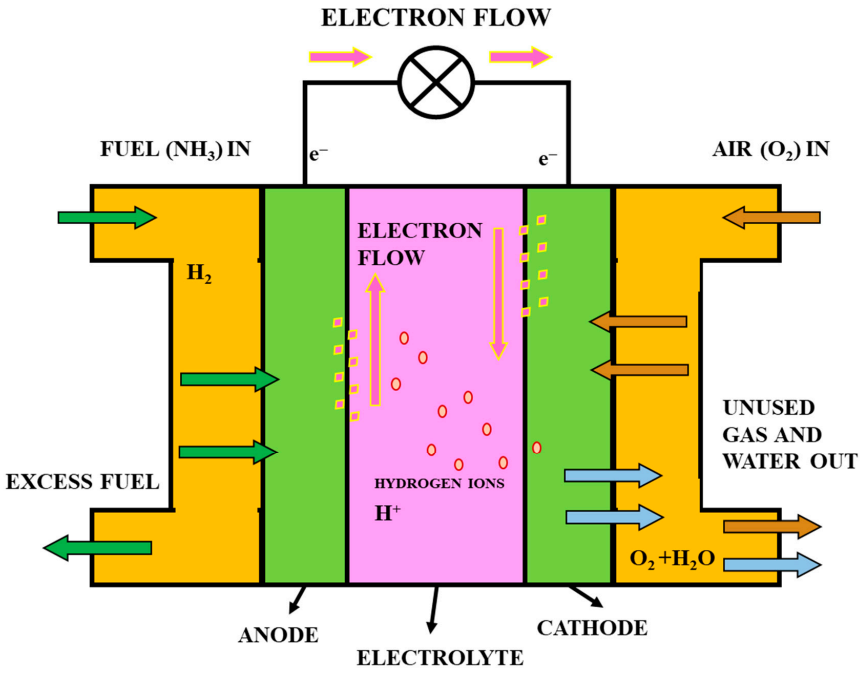

Figure 2. Schematic representation of ammonia-fueled H-SOFC [16]. NH_3 and air need to be supplied to the anode side and cathode side, respectively. The electrolyte in the middle conducts protons.

Likewise, water is formed as oxygen molecules at the cathode interact with incoming anode protons and electrons. The electrical energy is produced on the basis of the following chemical reactions;

Anode reaction:

$$3H_2 \rightarrow 6H^+ + 6e^-$$

Cathode reaction:

$$1.5\ O_2 + 6H^+ + 6e^- \rightarrow 3H_2O$$

Overall cell reaction:

$$4NH_3 + 3O_2 \rightarrow 6H_2O + 2N_2$$

The produced electrical energy is extracted from fuel cells with a continuous supply of fuel. To accelerate electrochemical reactions and facilitate the movement of gases and chemicals within the fuel cell, catalysts are utilized in electrochemical reactions. The comparison between SOFCs and other fuel cells is demonstrated in Table 1.

Table 1. List of different fuel cell types, along with their corresponding operating temperature, charge carrier, electrical efficiency, power output, potential applications, as well as their respective advantages and disadvantages [1,16].

Fuel Cell	Temperature (°C)	Charge Carrier	Efficiency (%)	Competent Power	Application	Advantages	Disadvantages
Alkaline fuel cell (AFC)	50–90	OH^-	50–70	10–100 KW	Aerospace applications	Less operating temperature and high efficiency	Toxic byproduct, illiberal to CO_2 in impure H_2 and air, corrosion, and expensive
Phosphoric acid fuel cell (PAFC)	175–220	H^+	40–45	10 MW	Energy needed in hospitals, schools, and offices	High efficiency and liberal to impure H_2	Corrosion and sulfur poisoning, low power density
Molten carbonate fuel cell (MCFC)	600–650	CO_3^{2-}	50–60	100 MW	Large-scale distributed commercial generation	High efficiency	Sulfur poisoning, electrolyte instability, and corrosion
Direct methanol fuel cell (DMFC)	50–120	H^+	25–40	100 KW to 1 MW	Mobile phones, laptops, and battery chargers	High power density, low temperature, and no reforming	Methanol crossover and byproduct poisoning, low efficiency
Polymer electrolyte membrane fuel cell (PEMFC)	60–100	H^+	40–50	100 W to 500 KW	Vehicles	Low temperature and high power density	Illiberal to CO in impure H_2 and expensive
Solid oxide fuel cell (SOFC)	800–1000	O^{2-}	50–60	100 MW	Residential and Factory	Direct fossil fuel and high efficiency	Thermal stress failure, high temperature, and sulfur poisoning
Protonic ceramic fuel cell (PCFC)	450–750	H^+	>50	25 KW	Heavy-duty trucking and remote power applications	Lower degradation, high conductivity, and less working temperature	More appropriate electrolyte and electrode materials needed and complex fabrication

2.1. Electrolyte Materials

To complete the chemical reactions, electrolyte materials transport the oxide and proton ions between the anode and cathode. At the cell operating temperature, the thick electrolyte will be stable and unreactive. Electrolyte materials also require similar coefficients of thermal expansion (CTE), high protonic ion conductivity, and low electronic conductivity. The yttria-stabilized zirconia (YSZ) demonstrates long-term stability in different environments and possesses high ionic conductivity that makes it suitable for use in oxygen ion-conducting solid oxide fuel cells (O-SOFCs). It is the most used and described material for O-SOFCs, but it needs a high operating temperature (800–1000 °C), which is its major drawback in rendering the cell degradation. At similar temperatures,

the conductivity of the H-SOFC electrolyte material is coherently lower than that of the O-SOFC material [17–19]. Stabilized ceria is another fluorite-type doping material that has good ionic conductivity at low operating temperatures and low polarization resistance in comparison with the YSZ. However, it demonstrates the low oxygen partial pressure during electronic conduction [20–23]. Strontium-doped lanthanum gallate (SDC) has higher ionic conductivity than YSZ, making it a promising option. It also operates at lower temperatures, which increases its potential for global commercialization [24,25].

Proton-conducting ceramic electrolytes provided good ionic conductivity at an intermediate temperature while using barium cerate ($BaCeO_3$), barium zirconate ($BaZrO_3$), and strontium cerate ($SrCeO_3$) doped by trivalent cations like Y, Yb, Pr, Sc, Nd, etc., combined with a Ni-based composite anode [26–28]. Protonic conducting electrolytes often have advantages over the corresponding oxide ion-conducting SOFCs, including cheaper connecting materials, better sealing and reliability, being economically attractive, having a lesser likelihood of material deterioration, and having excellent endurance, which resolves a material challenge shown in Figure 3.

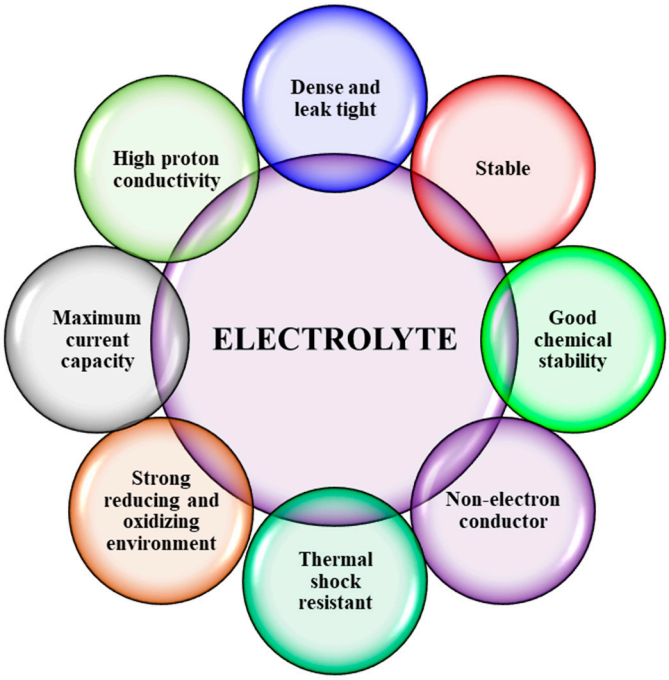

Figure 3. Essential properties of electrolytes to use in SOFCs [16].

2.2. Cathode Materials

Cathode materials are considered a bottleneck in reducing the operating temperature of SOFCs as the dominant active cathode polarization decreases the operating temperature [29–32]. The process in which air gets into the cathode and oxygen molecules are converted into oxides is called the oxygen reduction reaction (ORR). The oxygen reduction reaction usually occurs in the triple-phase boundary (TPB) present in oxide ion-conducting phases, electron-conducting phases, and air. For efficient oxygen reduction reaction (ORR), the cathode should possess the following:

- High surface area and compatibility with the electrolyte;
- Fairly high electron-conducting activity;
- Adequate porosity to support oxygen diffusion;
- Oxide ions should have high ionic conductivity.

TPB depends on the microstructure and material composition of the cathode [29]. The cathode also needs to have a similar thermal expansion coefficient (CTE) to the electrolyte to avoid thermal stress that could affect structural stability. Cathode materials should be chemically inert to electrolyte materials and stable in oxidizing situations. Lanthanum

strontium manganite (LSM), which is thermally compatible with electrolytes and other components, is regarded as an advanced cathode material for high-temperature SOFCs. Another option is the composite of LSM and YSZ to increase the electrochemically active field [29]. LSM is chemically stable at 1100 °C but reacts with YSZ if the temperature exceeds 1100 °C. For lower temperatures, the polarization resistance of LSM is high, making LSM unsuitable for intermediate-temperature SOFCs.

2.3. Anode Materials for SOFCs

Materials having various structures, such as perovskite, fluorite, rutile, spinel, and double perovskite, have been explored as anode materials. A comprehensive review has been conducted on various types of metal-fluorite cermet electrodes [33–35]. For instance, nickel (Ni) has been combined with YSZ, doped gadolinium ceria (GDC), doped samarium ceria (SDC), and Scandia-stabilized zirconia (SSZ). Additionally, saturated Ni with cerium (Ni-CeO_2) has been utilized with YSZ, while copper (Cu) and Ni have been employed with SDC [29], but Ni-YSZ is regarded as one of the most advanced materials among them [36–38]. Nickel exhibits effective electrochemical activity for hydrogen oxidation, as well as strong catalytic activity for reforming hydrocarbons and cracking ammonia. Ni-YSZ has a coefficient of thermal expansion (CTE) that is consistent with the electrolyte, and it extends the area for the electrochemical reaction of the triple-phase boundary (TPB) [29].

Due to the structural and compositional features, perovskite materials demonstrate useful potential for use in anodes [39]. For instance, Nickel-free perovskite materials with high sulfur tolerance, namely $La_{0.75}Sr_{0.25}Cr_{0.5}Mn_{0.5}O_3$ (LSCM) and $La_{0.75}Sr_{0.25}TiO_3$ (LST), have been developed. By utilizing a single-phase LSCM, the electrochemically active region is established at the solid–gas interface, thereby increasing the reactive area [29,40,41]. In the temperature range of 500–700 °C, Yang et al. [42] studied how ammonia is utilized in SOFCs and concluded that the ammonia is initially decomposed, and the resulting hydrogen is preferred over the direct electro-oxidation of ammonia for the electrochemical reaction at the anode. Anode material should possess the following characteristics:

- It should have sufficient porosity, conductivity, and chemical and mechanical stability properties;
- It should have electrochemical activity and fuel flexibility properties;
- It should have strong catalytic activity to promote the reaction of the fuel with oxide ions;
- It should have low polarization resistance of the electrode.

3. Role of Numerical Modeling

In the last few decades, much importance has been imposed on the development of precise models for the various phenomena happening in SOFCs, and this has produced a huge number of publications in this field. For the complexity of the three-dimensional fuel cell modeling, much work has been performed by computational fluid dynamics, which is typically numerical modeling. It is really important to find out the temperature distribution through the cell since the operating temperature affects the ohmic polarization, activation polarization, thermal stress, and concentration polarization inside the cell. In order to account for electrochemical effects and ohmic heating, solving the energy equation with all associated source terms is essential in order to determine the temperature distribution in SOFCs, and one of the most important parameters that needs to be set perfectly is the thermal boundary condition. Numerical modeling is an effective tool for analyzing the fluid domain and dealing with mechanical stress analysis through the SOFCs. It also has various advantages for ammonia-fueled H-SOFCs over experimental studies since parametric analysis can be performed easily in an efficient and cost-effective way rather than doing experiments in a laboratory. Furthermore, numerical analysis can be performed easily to characterize the complex effect of physical phenomena like ion or electron transport, gas transport, and electrochemical reactions in SOFCs [43]. Numerical modeling can also execute those tasks that cannot be performed well by experiments, such as the dispersion

of gas composition and temperature in the micro-structured SOFCs. For performing these types of complex measurements, numerical modeling is effective.

Numerical models implemented in commercial COMSOL Multiphysics [44] can solve the various types of faults inside the SOFCs, which is very helpful to the researchers in studying the cell operations under normal and faulty conditions to understand the new strategic design. COMSOL Multiphysics is not limited to planar only but uses tubular geometries to understand the cell properly [44]. Ilbas et al. [10] used a 3D numerical model in COMSOL Multiphysics to conduct the comparative performance analysis of a flat tubular anode-supported ammonia-fueled SOFC. COMSOL Multiphysics can be used to model the H-SOFC performance parameters such as cell diameter, polarization, concentration, porosity, thickness, and thermal stress in order to determine the performance of the ammonia-fueled H-SOFC. Numerical modeling in COMSOL Multiphysics is described as follows and shown in Figure 4:

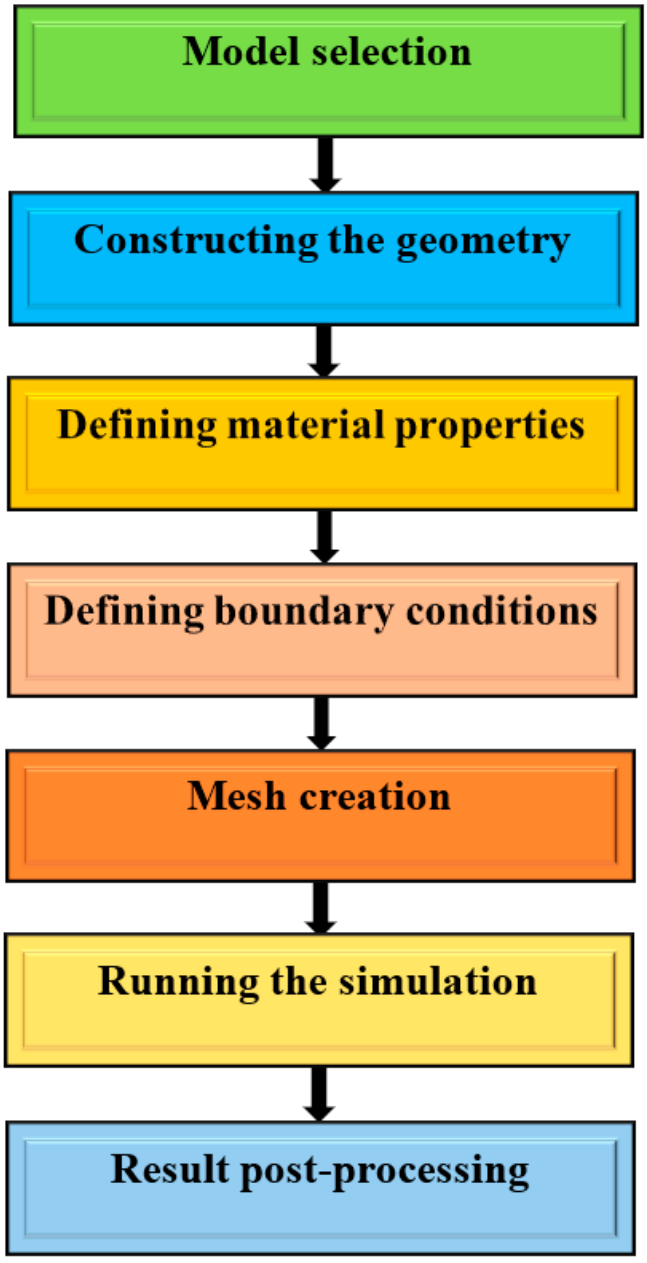

Figure 4. Flow chart for numerical methodology.

3.1. Application of Numerical Modeling in Ammonia-Fueled H-SOFC

The zero-dimensional cell model is unable to describe the higher dimensional variables, such as two or three-dimensional variables, over SOFC components such as the anode, cathode, electrolyte, or current collectors. This type of model may produce output parameters like voltage output, power density, and cell efficiency under a certain set of input parameters. The one-dimensional models ignore the other spatial dimensions and represent the process variables of fuel cell components in a single direction. It is capable of simulating counter-flow and co-flow cell configurations but is unable to simulate cross-flow systems. But, the models that are two-dimensional (2D) or three-dimensional (3D) can render the spatial distribution of variables, which includes cross-flow over the fuel cell components. For constructing the 2D and 3D models of cell configuration, computational fluid dynamic techniques are generally used that can be solved numerically or analytically. But, the analytical solutions are not always as quick and effective as the numerical ones. Instead of applying analytical techniques, numerical procedures may be applied to obtain faster solutions. Recently, notable research attempts have been made towards developing electrolyte materials for ammonia-fueled H-SOFCs. This is due to the fact that the higher ohmic overpotential of H-SOFCs does not provide a significant performance improvement. So, a more suitable model is essential in the development of ammonia-fueled H-SOFCs. We have analyzed the recent numerical modeling based on the ammonia-fueled H-SOFC and the associated partial differential equations that govern the numerical modeling.

3.2. Recent Ammonia-Fueled SOFC Models

The main purpose of the proton conducting electrolyte-supported SOFC is to attain optimal power density at intermediate temperatures. Running the SOFC at high temperatures can lead to thermal stress on the electrolyte. However, by employing ammonia as the fuel, which decomposes at intermediate temperatures, this issue can be avoided during experimentation. Before conducting large-scale experiments, it is essential to develop a universal model adaptable to all kinds of SOFCs to achieve the highest power density while utilizing ammonia as fuel.

Ilbas et al. [10] studied the efficiency of a 3D model of a flat tubular solid oxide fuel cell with a direct ammonia-fed anode. Isothermal temperature distribution and co-flow of reactant gases were taken into consideration. The subsystem of the model incorporated uniform velocities, fluid viscosity, and partial pressure. The simulation was conducted under steady-state conditions, maintaining an ideal airflow. Their findings indicated that when operating under the same parameters and geometries, the model with a direct ammonia-fed anode showed superior performance compared to the hydrogen-fed model. Additionally, their research confirmed that when applying the same active cell surface area, gas channel length, and operating conditions, the direct ammonia-fed anode-supported flat-tubular SOFC demonstrated better performance when compared to the corresponding anode-supported tubular SOFC. Figure 5a,b shows the flat-tubular SOFC and its performance. Asmare et al. [12] studied the usefulness of micro-tubular solid oxide fuel cells fueled by ammonia as a possible source for eco-friendly and sustainable power generation, as described in Figure 5c,d. Laminar flow was taken into account, with the reactants assumed to be ideal and incompressible gases. The evaluation of the model's effectiveness was performed through analysis of the Brinkman, incompressible Navier–Stokes, and Butler–Volmer equations. Their research revealed that the numerical power densities obtained by direct hydrogen, ammonia, and experimental use of pure hydrogen were 622.29 mW/cm^2, 628.92 mW/cm^2, and 589.28 mW/cm^2, respectively, at the same geometric combination and parameter size.

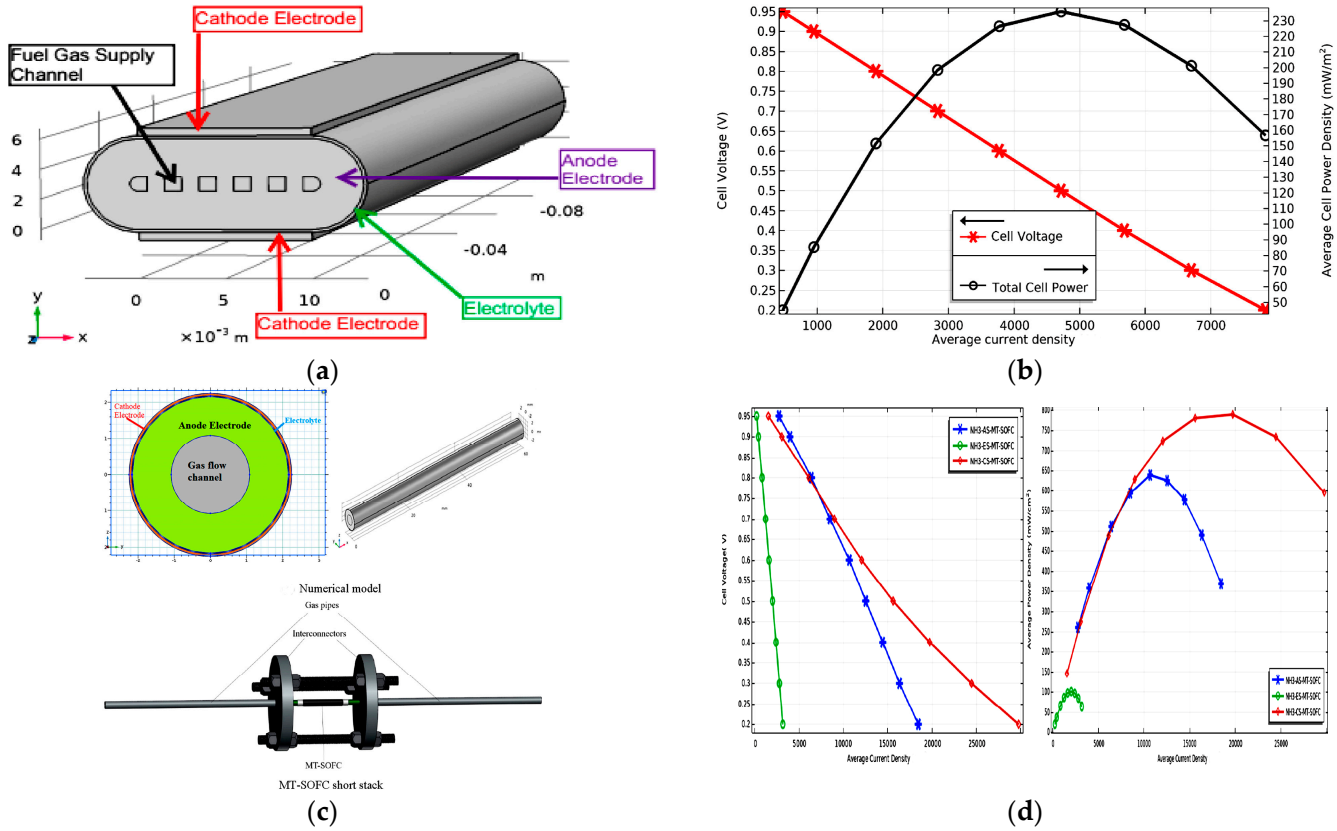

Figure 5. (**a**) Schematic representation of anode-supported flat tubular SOFC and (**b**) direct ammonia-fueled anode-supported flat tubular SOFC polarization curve (red line) and power curve (black line) at 1073 K, reproduced with consent from reference [10], copyright 2022, Elsevier. (**c**) Schematic representation of micro-tubular SOFC and (**d**) polarization and power curve for the performance comparison of electrolyte and electrode-supported ammonia-fueled micro-tubular SOFC, reproduced with consent from reference [12], copyright 2022, Elsevier.

Wang et al. [2] reviewed direct ammonia fuel cell and electrochemical synthesis for a green energy carrier. According to their study, ammonia has emerged as a highly favorable choice for hydrogen storage and is recognized as an environmentally friendly energy carrier, as demonstrated in Figure 6a,b. In addition, ammonia demonstrates crucial advantages in long-distance passage. The performances, prospects, and limitations of direct ammonia-fueled thin film SOFCs were studied by Oh et al. [11]. Their study showed a significant difference in the performance of H_2 and NH_3 as fuel. A higher current density was achieved while using NH_3 as fuel, as depicted in Figure 6c,d.

A study on the mathematical modeling of direct internal reforming solid oxide fuel cells (SOFCs) with the goal of developing a feasible design and optimizing the operating conditions was conducted by Faheem et al. [45]. Volume-averaging and microstructure-oriented mathematical approaches were discussed in their study. The volume-averaging model integrates equations related to the bulk properties of transport phenomena, while the microstructure numerical model takes into account the impact of electrode heterogeneity. They explored the multiscale mathematical modeling techniques and analyzed the impacts of both electrochemical and chemical reactions. Afif et al. [8] carried out a comparative study on ammonia fuel cells to review the suitability of using ammonia in next-generation direct ammonia-fed SOFCs. Ni [46] conducted a study on a planar SOFC that used ammonia as fuel to investigate mass/heat transfer and electrochemical and chemical reactions. Laminar flow conditions were taken into account to describe transport phenomena due to the small Reynolds number of the fluid flow. The study resulted in the development of a 2D model presented in Figure 7a–c. Their findings revealed that an augmentation in the inlet

temperature of the ammonia-fueled SOFC led to a higher electrical output. However, it is worth noting that the temperature gradient near the inlet of the SOFC was considerably high. Ni et al. [43] studied the mathematical model and experimental work of SOFCs fueled by ammonia and concluded that ammonia can be directly applied as a feasible fuel in SOFCs.

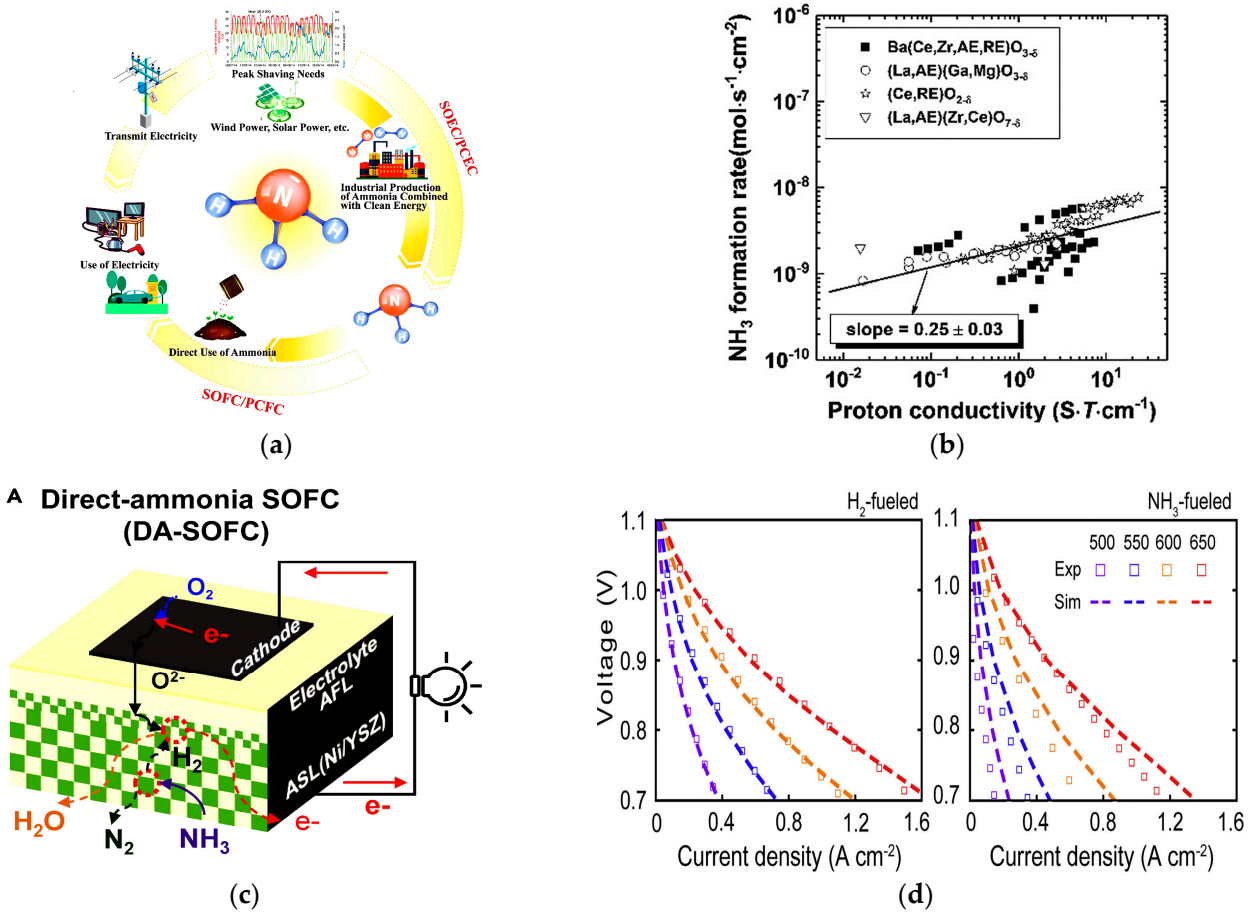

Figure 6. (**a**) Energy carrier model of ammonia (**b**) proton conductivity of the electrochemical ammonia formation rate for selected electrolytes at 623–923 K, reproduced with consent from reference [2], copyright 2022, Elsevier. (**c**) Operating rule of direct ammonia SOFC and (**d**) IV curve comparison between experiment and simulation result of H_2-fueled and NH_3-fueled SOFC. Reproduced from reference [11], open access.

Wojcik et al. [47] conducted a relative study between the performance and outcomes of a solid oxide fuel cell using hydrogen and ammonia as fuel. The results indicated that ammonia is a promising option for SOFCs, as illustrated in Figure 7d–f. Ilbas et al. [48] investigated the potentiality of tubular SOFCs with ammonia as a fuel in the anode, cathode, and electrolytes. Fundamental boundary conditions, including velocity non-slip conditions and the negligible influence of gas flow boundary layers, were considered. The governing equations encompassed aspects of charge, species, momentum, energy, concentration, and mass conservation, all coupled with the electrochemical reaction of ammonia. Their findings demonstrated that ammonia may be used as a carbon-free fuel for tubular SOFCs and also revealed that SOFCs with cathode support provide better performance compared to those with anode or electrolyte support. Rathore et al. [29] reviewed SOFC technologies directly fueled with ammonia for the purpose of experimental and numerical studies and discussed the challenges of anode-supported SOFCs versus hydrogen-fueled SOFCs through modeling.

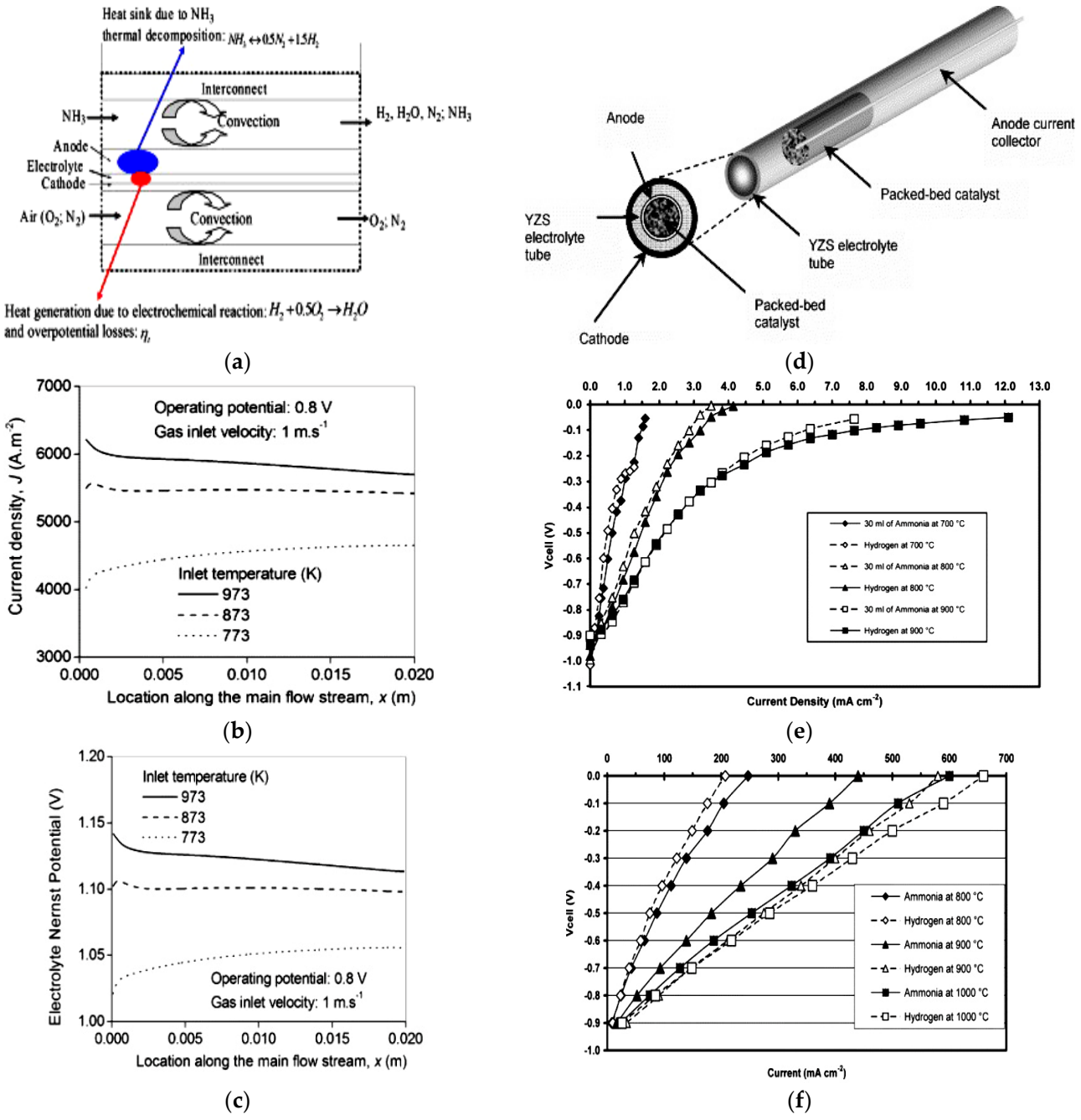

Figure 7. (**a**) Heat sink and heat generation of NH_3-fueled SOFC, (**b**) temperature effect on NH_3-fueled SOFC for current density distribution, and (**c**) temperature effect on NH_3-fueled SOFC for electrolyte Nernst potential distribution; reproduced with consent from reference [46], copyright 2011, Elsevier. (**d**) Schematic of fuel cell model depicting packed bed catalyst in situ in the electrolyte tube, (**e**) comparing NH_3 and equivalent H_2 fuel at various temperatures for silver anode with in situ iron catalyst, and (**f**) comparing NH_3 and equivalent H_2 fuel at various temperatures for a platinum cell without additional catalyst; reproduced with consent from reference [47], copyright 2003, Elsevier.

Asmare et al. [13] investigated the properties of an ammonia-fueled anode-supported proton conducting SOFC for comparison with a hydrogen-fueled SOFC and an ammonia-fueled oxygen-ion conducting SOFC under the same operating parameters and geometries. The PEN structure was taken into account, employing a co-flow arrangement with a constant operating temperature for the cells. The model was supplied with ammonia at the anode and air at the cathode, both flowing in a laminar manner under steady-state

conditions. The reactant gases were treated as ideal and incompressible. They showed that ammonia-fueled tubular cells are strongly influenced by anode position, pressure, and operating temperature in both electrolytes, although cell temperature effects are greater in proton-conduction cells, as shown in Figure 8. Valera-Medina et al. [9] carried out a comprehensive analysis of ammonia as a potential fuel, exploring both its advantages and limitations in terms of storing energy from renewable sources. Their review provides a comprehensive overview of the advancements in each aspect of using ammonia as an energy carrier. Table 2 illustrates the comparison of different models with their analysis for ammonia-fueled SOFCs applications, and Table 3 gives the different numerical methods used for ammonia-fueled SOFC modeling.

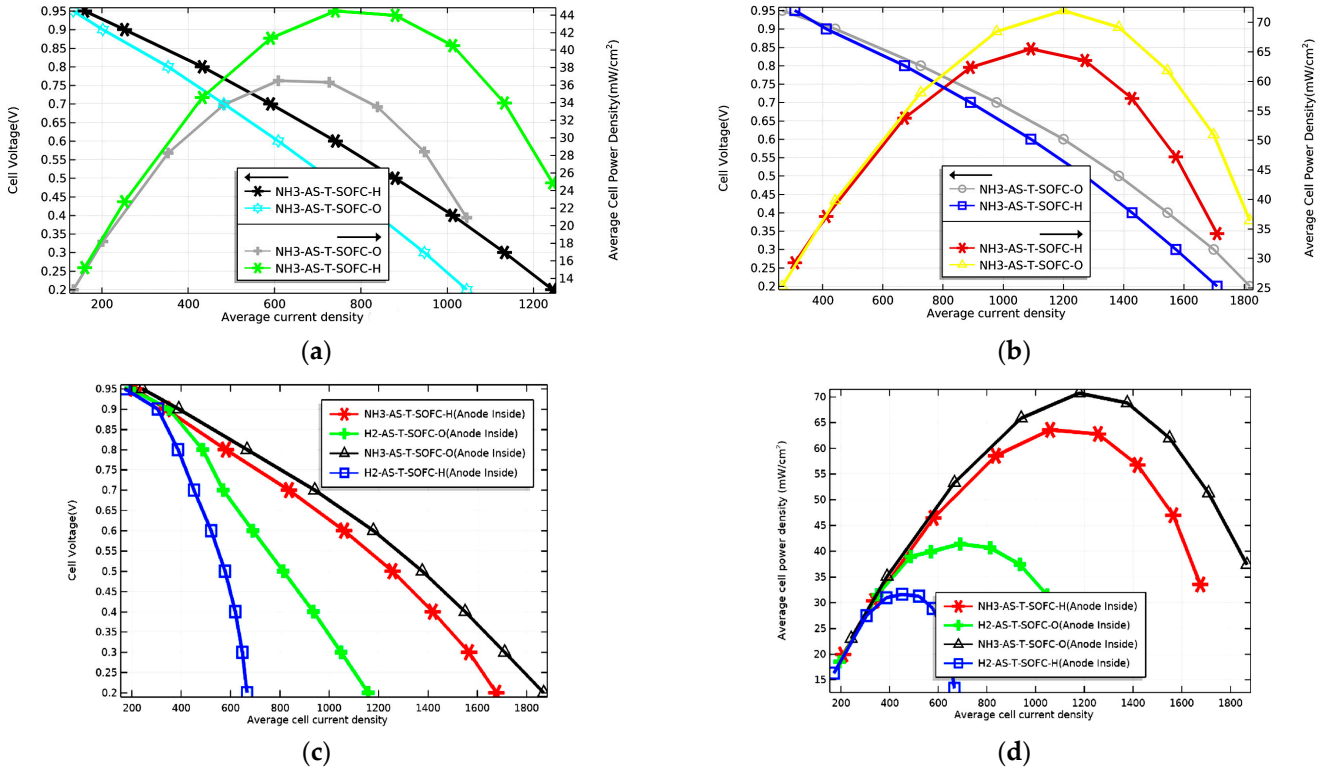

Figure 8. (**a**) Polarization and power curve of NH_3-fueled anode-supported tubular SOFC at 973 K, (**b**) polarization and power curve of NH_3-fueled anode-supported tubular SOFC at 1073 K, (**c**) polarization comparison of direct NH_3- and H_2-fueled tubular SOFCs using different electrolytes and anode position at 1073 K, and (**d**) power density comparison of direct NH_3- and H_2-fueled tubular SOFCs using different electrolytes and anode position at 1073 K; reproduced with the permission from reference [13], copyright 2021, Elsevier.

Table 2. Comparison of different models with their analysis for ammonia-fueled SOFCs.

Description of Model	Analysis of Model
Anode-supported flat tubular SOFC using ammonia fuel [10]	A three-dimensional modeling approach was explored for an anode-supported flat tubular SOFC. Comparative analysis revealed that the performance of the anode-supported flat tubular SOFC exceeded that of the tubular SOFC at high temperatures. However, no simulations were conducted for intermediate temperatures, which are of utmost importance for minimizing cell degradation. Moreover, no findings are available regarding cell performance when cathode concentration remains constant.

Table 2. *Cont.*

Description of Model	Analysis of Model
A thin film SOFC performance using ammonia fuel [11]	An intermediate temperature (923 K) was considered for this experiment, which found the highest density (1330 mW/cm^2). However, the influence of active catalysts with suitable diffusion channels within the SOFC was not taken into consideration. The optimization of the diffusion process has the potential to substantially enhance the performance of ammonia-fueled SOFCs, enabling them to attain a performance level comparable to that of hydrogen-fueled cells.
A thermo-electrochemical model was developed for ammonia-fueled planar SOFC [46]	SOFCs typically exhibit higher electric potential. However, in this specific model, achieving higher electric potential at intermediate temperatures was not possible due to the requirement for a higher temperature gradient. Higher temperature also causes thermal stress in SOFCs. Furthermore, the model did not definitively determine whether a low inlet velocity or a high inlet velocity is more appropriate for the ammonia-fueled SOFC.
Electrolyte and electrode-supported tubular SOFC was discussed for fuel comparison [48]	Cathode-supported ammonia-fueled SOFCs revealed better performance than anode and electrolyte-supported ones in high temperatures. But, an intermediate temperature was not considered for the modeling. Furthermore, in cases when the anode is positioned within the inner part of the tube, there is no conclusive evidence regarding high concentration losses due to low diffusion at the cathode.

Table 3. List of different numerical methods used for ammonia-fueled SOFC modeling [49].

Method	Description	Advantages	Disadvantages
Finite Difference Method (FDM)	The FDM is a straightforward approach to discretizing the governing equations on a grid and approximate derivatives using finite differences. It is relatively simple to implement and suitable for regular geometries. The FDM is often used for steady-state and transient simulations of SOFCs.	The notable strength of the finite difference method lies in its adaptability to represent intricate geometries and diverse material characteristics. This adaptability renders it applicable across a broad spectrum of scenarios, enabling the treatment of varied problems and systems. Furthermore, the finite difference method facilitates the computation of transfer functions and supports acoustic analysis pertaining to intricate structural configurations [50].	The major drawback is the computational strength of the calculations, especially when fine sampling is required on both horizontal and vertical grids. This can lead to enhanced computational time and resource requirements, particularly for large-scale problems. As a consequence, the finite difference method might not be the most efficient choice for certain applications where computational efficiency is more important [50].
Finite Volume Method (FVM)	The FVM involves discretizing the domain into control volumes and solving the conservation equations for mass, momentum, energy, and species within each volume. The FVM is known for its conservation properties and is widely used for modeling fluid flow and heat transfer in SOFCs.	The Finite Volume Method inherently conserves quantities within control volumes, making it suitable for problems involving conservation laws. This ensures an accurate representation of physical processes. It naturally handles source terms within control volumes, ensuring proper incorporation of external influences or internal generation of quantities. For example, the FVM has become very promising for solving elliptic boundary value problems where it needs to follow the conservation of law principle [51].	Implementing the FVM can be complex, especially for problems involving non-orthogonal grids or complex boundary conditions. Proper intervention of boundary conditions can be challenging and may require specialized techniques [51].

Table 3. *Cont.*

Method	Description	Advantages	Disadvantages
Finite Element Method (FEM)	The FEM is versatile and can handle complex geometries with ease. It subdivides the domain into finite elements, allowing for an accurate representation of irregular shapes. The FEM is often used for structural analysis and can also be extended to solve the fluid flow and heat transfer equations.	The FEM is well suited for handling complex geometries and irregular domains. It can efficiently model structures with intricate shapes or irregular boundaries. It can achieve high accuracy by using higher-order elements, allowing for better representation of curved or intricate solutions. The FEM naturally integrates boundary conditions, including essential (Dirichlet) and natural (Neumann) boundary conditions, making it suitable for problems involving external constraints [12].	Solution accuracy can be sensitive to the quality and density of the mesh. Fine meshes can improve accuracy but may lead to higher computational costs. Some problems can result in ill-conditioned matrices, affecting the stability and convergence of the numerical solution. For certain time-dependent problems, the FEM might require substantial computational resources due to the transient nature of the solution [48].
Lattice Boltzmann Method (LBM)	The LBM is a mesoscopic method based on the kinetic theory of gases. It is particularly suitable for simulating complex fluid flows with porous media, such as the electrodes in SOFCs. The LBM can handle multiphase and multiscale phenomena effectively.	The LBM is well suited for high-performance computing architectures, allowing for efficient simulations of large-scale problems. Boundary conditions can be implemented naturally by incorporating bounce-back schemes, making it straightforward to handle various flow conditions and geometries. It can handle irregular and complex geometries with relative ease, as the method's discrete lattice structure simplifies boundary treatment and mesh generation [52].	While the LBM has seen significant development and application, it might not be as mature as other established methods like finite volume or finite element methods, particularly for certain types of problems. It might face challenges in accurately simulating flows with high Reynolds numbers or strong turbulence, as the lattice structure and inherent viscosity can impose limitations on turbulent flow modeling. Achieving high accuracy in LBM simulations often requires fine spatial and temporal resolutions, which can lead to increased computational costs [52].
Smoothed Particle Hydrodynamics (SPH)	SPH is a Lagrangian particle-based method used for simulating fluid dynamics. It is well suited for problems involving large deformations and fluid–structure interactions. SPH can be applied to simulate fluid flow and heat transfer within SOFCs.	SPH is well suited for simulations of complex geometries, as it does not require structured grids. This makes it particularly useful for problems like fluid–structure interactions and multiphase flows, where the boundaries are complex and may change over time. It can handle free surface simulations, making it useful for simulating flows with distinct interfaces between different phases, such as water and air or liquid droplets in a gas environment. Since SPH is a Lagrangian method, meaning that each particle moves with the fluid, and its motion is tracked individually. This is favorable for capturing fluid movement and deformation accurately, especially in cases where Eulerian methods might struggle, such as highly turbulent or chaotic flows [53].	Properly imposing boundary conditions in SPH simulations can be challenging. The smoothing kernels used in SPH can lead to inaccuracies near boundaries, which can affect the simulation results since SPH does not rely on structured grids, which can lead to some difficulties in interpolating properties between particles [53].

Table 3. *Cont.*

Method	Description	Advantages	Disadvantages
Boundary Element Method (BEM)	The BEM is useful for problems with boundary-dominated phenomena, such as heat conduction through thin structures like SOFC electrolytes. It discretizes only the boundary of the domain, reducing the computational effort compared to volume-based methods.	The BEM solves problems on the boundary, resulting in lower-dimensional integrals compared to volume-based methods like the Finite Element Method (FEM). It is well equipped to handle potential singularities in the governing equations, such as when dealing with Laplace or Helmholtz problems, and is suitable for problems involving unbounded or semi-infinite domains, such as acoustic or electromagnetic scattering problems. It only requires discretizing the boundary, making it advantageous for such scenarios [54].	The BEM lacks a traditional mass matrix like the FEM, making it less suitable for transient or dynamic problems where mass effects are substantial. Time-domain analysis can be more involved in the BEM. Mesh adaptation and refinement can also be challenging [54].
Molecular Dynamics (MD) and Monte Carlo (MC) Methods	MD and MC methods are used at the molecular scale to study interactions between atoms and molecules. They can be employed to analyze surface reactions, adsorption, and diffusion of species on electrode surfaces and within the electrolyte.	MD simulates the time evolution of a system's particles, providing insights into the dynamic behavior of molecules and their interactions. It captures temporal evolution, equilibration, and dynamic processes. It accurately conserves energy and momentum, obeying the laws of mechanics. This allows for the study of energy fluctuations and transport properties, which are essential for understanding thermodynamics. MC methods provide statistically accurate sampling of configuration space, enabling the calculation of thermodynamic properties. It does not have inherent time-step limitations, making it suitable for simulating processes with a wide range of timescales [55].	MD simulations are typically limited to picoseconds to microseconds, restricting the study of slower processes or long-term phenomena. It depends on empirical force fields, which may have limitations in accurately describing certain molecular interactions. MC simulations are subject to systematic errors, including finite-size effects and discretization errors. It uses discrete moves to explore configuration space, which can limit the accuracy of sampling, particularly in high-dimensional spaces [55].
Coupled Methods	Combining different numerical methods can provide more accurate and efficient solutions. For instance, coupling FEM with FVM or FDM can be used to model the coupled fluid flow, heat transfer, and electrochemical reactions in SOFCs.	Coupled methods enable multiscale simulations, where different simulation techniques are applied to different lengths or timescales. This is important for studying systems with multiple interacting processes occurring at different scales. It can enhance accuracy by incorporating higher-fidelity simulations for specific regions or components of a system and help to identify potential limitations in the individual methods [56].	Coupled simulations can encounter numerical stability and convergence issues, especially when transferring information between different simulation domains or grids. Developing and maintaining coupled software can be complex and time-consuming [56].
Hybrid Methods	Hybrid methods combine continuum-based approaches (such as FVM or FEM) with particle-based methods (such as SPH or LBM) to capture different lengths and timescales within the system.	Hybrid methods enable multiscale simulations, allowing the study of systems with multiple lengths and timescales. It can significantly reduce the overall computational cost compared to fully resolving the entire system with a single high-fidelity method [57].	Hybrid methods frequently involve assumptions and approximations when transitioning between different methods. It is difficult to ensure accuracy at the interfaces and minimize errors [57].

3.3. Governing Mathematical Equations Used in Ammonia-Fueled H-SOFC

Ammonia decomposition is presumed at the porous anode, and the rate of ammonia decomposition is defined as [29]

$$r = 4 \times 10^{15} \exp\left(-\frac{196200}{RT}\right) P_{NH_3} \quad (1)$$

P_{NH_3} denotes the partial pressure of ammonia, R is the ideal gas constant (8.314 $Jmol^{-1}K^{-1}$), T is the operating temperature, and 196,200 KJ/mol is the activation energy.

The Nernst equation can be used to express the utmost theoretical voltage of an NH_3-fueled SOFC based on a thermodynamic analysis that compares the maximum performance of NH_3-fueled H-SOFCs and O-SOFCs [43],

$$E_{\text{Nernst}} = -\frac{\Delta G}{nF} - \frac{RT}{nF} \ln\left[\frac{P_{H_2O}}{\left(P_{O_2}\right)^{\frac{1}{2}} P_{H_2}}\right] \quad (2)$$

where ΔG = Gibbs free energy of water formation reaction (186 KJ/mole), P_{H_2} = partial pressure of hydrogen, P_{O_2} = partial pressure of oxygen, P_{H_2O} = partial pressures of steam, n = number of electrons transferred during reaction, R = ideal gas constant (8.314 $Jmol^{-1}K^{-1}$), T = operating temperature (K), and F = Faraday constant (96,485 $Cmol^{-1}$).

The actual voltage of the cell is less than the open circuit voltage (OCV) due to the irreversible losses of the electrode, including ohmic, concentration, and activation polarization. The actual cell voltage is expressed as

$$V_{\text{cell}} = E_{\text{Nernst}} - (\eta_{\text{act}} + \eta_{\text{ohm}} + \eta_{\text{conc}}) \quad (3)$$

In Equation (2), E_{Nernst} = theoretical OCV and η_{act}, η_{ohm}, and η_{conc} denote the activation, ohmic, and concentration polarizations, respectively.

Ohmic overpotential originates from the ohmic losses that happen in the cell's electrodes, electrolyte, and current collectors [29]. Ohmic losses are, therefore, expressed as

$$\eta_{ohm} = jR_e d_e \quad (4)$$

where R_e and d_e denote the resistivity and thickness of the electrolyte, respectively.

The activation polarizations in the electrodes are assessed by the Butler–Volmer equation [58]. The activation polarization of electrodes is determined by the following:

$$i_{an} = i_{0,an}\left(e^{\frac{\beta_{an} n F \eta_{act,an}}{RT}} - e^{\frac{-(1-\beta_{an}) n F \eta_{act,an}}{RT}}\right) \quad (5)$$

$$i_{ca} = i_{0,ca}\left(e^{\frac{\beta_{ca} n F \eta_{act,ca}}{RT}} - e^{\frac{-(1-\beta_{ca}) n F \eta_{act,ca}}{RT}}\right) \quad (6)$$

where i_{an} = anode current density, i_{ca} = cathode current density, $i_{0,an}$ = anode exchange current density, $i_{0,ca}$ = cathode exchange current density, β = symmetric factor, n = transferred number of electrons, and $\eta_{act,an}$, $\eta_{act,ca}$ = anode and cathode activation polarization.

Concentration polarization occurs in the electrodes due to the resistance of reactant transport and the product species at the electrochemically active sites [29]. This phenomenon is described by the concentration difference between the surface and electrolyte interface of the electrode [59]. The concentration polarization of H-SOFCs is expressed as follows:

$$\eta_{conc \to a} = \frac{RT}{2F} \ln\left(\frac{P_{H_2}^M}{P_{H_2}^N}\right) \quad (7)$$

$$\eta_{conc\to c} = \frac{RT}{2F}\ln\left(\frac{\left(P_{O_2}^{M}\right)^{0.5}P_{H_2O}^{N}}{\left(P_{O_2}^{N}\right)^{0.5}P_{H_2O}^{M}}\right) \tag{8}$$

where $P_{H_2}^{N}$ = hydrogen concentration at anode electrolyte, $P_{H_2}^{M}$ = hydrogen concentration at anode surface, $P_{O_2}^{N}$ = cathode electrolyte's oxygen concentration, $P_{H_2O}^{N}$ = cathode electrolyte's steam concentration, $P_{O_2}^{M}$ = cathode surface's oxygen concentration, and $P_{H_2O}^{M}$ = cathode surface's steam concentration.

Some dynamic equations in mathematics, such as energy, momentum, continuity, and chemical species, are used in the 3D numerical model. To obtain comprehensive flow results, these equations should be solved concurrently for known boundaries, domains, and initial values. By making logical assumptions, these equations might be reduced and streamlined. The fundamental mathematical equations that govern 3D numerical modeling are summarized below [10].

Equations of Charge Conservation:

$$\nabla.i_{i0} = \Phi_{io}, i_{i0} = -\delta_{io}.\nabla\cdot\Phi_{io}, \nabla\cdot i_{el} = \Phi_{el}, i_{el} = -\delta_{el}.\nabla\cdot\Phi_{el} \tag{9}$$

where Φ_{i0} and Φ_{el} are the ionic and electronic potential, respectively; i_{i0} denotes the ionic charge and i_{el} represents the electronic charge.

Equation of continuity:

$$\frac{\partial(\rho u)}{\partial x} + \frac{\partial(\rho v)}{\partial y} + \frac{\partial(\rho w)}{\partial z} = S_m \tag{10}$$

where $S_m = \frac{i\left(M_{H_2O}-M_{H_2}\right)}{2F\Delta x}$ = anode electrolyte interface and $S_m = \frac{iM_{O_2}}{4F\Delta x}$ = cathode electrolyte interface.

Since the electrochemical reactions and transport processes in SOFCs can be relatively slow compared to the fluid flow dynamics, steady-state simulations are reasonable approximations to model the cell's behavior accurately. They require less computational effort and time compared to transient simulations. SOFCs are complex systems with complex geometries, and solving transient CFD simulations can be computationally expensive. By using steady-state simulations, faster results can be obtained while still capturing important aspects of the fuel cell's operation. It reveals important issues like temperature gradients, fuel depletion, and flow imbalances.

Momentum Equation:

$$\frac{\partial(\rho uu)}{\partial x} + \frac{\partial(\rho uv)}{\partial y} + \frac{\partial(\rho uw)}{\partial z} = -\frac{\partial p}{\partial x} + \frac{\partial}{\partial x}\left(\mu\frac{\partial u}{\partial x}\right) + \frac{\partial}{\partial y}\left(\mu\frac{\partial u}{\partial y}\right) + \frac{\partial}{\partial z}\left(\mu\frac{\partial u}{\partial z}\right) + S_x \tag{11}$$

$$\frac{\partial(\rho vu)}{\partial x} + \frac{\partial(\rho vv)}{\partial y} + \frac{\partial(\rho vw)}{\partial z} = -\frac{\partial p}{\partial y} + \frac{\partial}{\partial x}\left(\mu\frac{\partial v}{\partial x}\right) + \frac{\partial}{\partial y}\left(\mu\frac{\partial v}{\partial y}\right) + \frac{\partial}{\partial z}\left(\mu\frac{\partial v}{\partial z}\right) + S_y \tag{12}$$

$$\frac{\partial(\rho wu)}{\partial x} + \frac{\partial(\rho wv)}{\partial y} + \frac{\partial(\rho ww)}{\partial z} = -\frac{\partial p}{\partial z} + \frac{\partial}{\partial x}\left(\mu\frac{\partial w}{\partial x}\right) + \frac{\partial}{\partial y}\left(\mu\frac{\partial w}{\partial y}\right) + \frac{\partial}{\partial z}\left(\mu\frac{\partial w}{\partial z}\right) + S_z \tag{13}$$

where $S_x = \frac{\mu u}{K}$, $S_y = \frac{\mu v}{K}$, and $S_z = \frac{\mu w}{K}$.

Energy Equation:

$$\partial\left(\frac{\rho c_p uT}{\partial x}\right) + \partial\left(\frac{\rho c_p vT}{\partial y}\right) + \partial\left(\frac{\rho c_p wT}{\partial z}\right) = \frac{\partial}{\partial x}\left(\lambda\frac{\partial T}{\partial x}\right) + \frac{\partial}{\partial y}\left(\lambda\frac{\partial T}{\partial y}\right) + \frac{\partial}{\partial z}\left(\lambda\frac{\partial T}{\partial z}\right) + S_T \tag{14}$$

where $S_T = r_{NH_3} H_{NH_3}$ at the anode electrode and $S_T = i\left(\frac{T\Delta S}{2Ft_{ely}} + \frac{\eta}{t_{ely}}\right)$ at the electrolyte.

Chemical species:

$$\partial\left(\frac{\rho u Y_i}{\partial x}\right) + \partial\left(\frac{\rho v Y_i}{\partial y}\right) + \partial\left(\frac{\rho w Y_i}{\partial w}\right) = \frac{\partial}{\partial x}\left(D_{ij}\frac{\partial Y_i}{\partial x}\right) + \frac{\partial}{\partial y}\left(D_{ij}\frac{\partial Y_i}{\partial y}\right) + \frac{\partial}{\partial z}\left(D_{ij}\frac{\partial Y_i}{\partial z}\right) + S_{sp} \quad (15)$$

where $S_{sp,H_2} = \frac{-i}{2F} M_{H_2}$, $S_{sp,O_2} = \frac{-i}{4F} M_{O_2}$, and $S_{sp,H_2O} = \frac{i}{2F} M_{H_2O}$ in the above equations, ρ = reactant species density, t_{ely} = electrolyte thickness, ΔS = entropy changes during electrochemical reaction, μ = gas viscosity, S_T = volumetric heat source, S_m = source terms representing mass consumption and production during the electrochemical reaction of TPB, S_x, S_y, and S_z = source term of momentum and u, v, and w = velocity in the x, y, and z axes, respectively.

To make the above partial differential equations (PDE) dimensionless, the tentative following equations (Equations (15)–(17)) are described as follows:

$$\mathrm{Re} = \frac{\rho L u}{\mu} \quad (16)$$

where Re = Reynolds number, ρ = fluid density ($\mathrm{Kgm^{-3}}$), L = characteristic length (m), u = fluid speed ($\mathrm{ms^{-1}}$), and μ = dynamic viscosity of fluid ($\mathrm{Kgm^{-1}\ s^{-1}}$).

$$\mathrm{Pr} = \frac{\mu c_p}{\kappa} \quad (17)$$

where Pr = Prandtl Number, μ = dynamic viscosity of fluid ($\mathrm{Kgm^{-1}\ s^{-1}}$), c_p = specific heat($\mathrm{Jkg^{-1}k^{-1}}$), and κ = thermal conductivity ($\mathrm{Wm^{-1}K}-1$).

$$\mathrm{Nu} = \frac{hL}{\kappa} \quad (18)$$

where Nu = Nusselt number, L = characteristic length (m), and κ= thermalconductivity$\left(\mathrm{Wm^{-1}k^{-1}}\right)$.

Species diffusivity of the gas phase is described as

$$D_{i,j}^{eff} = \frac{\varepsilon}{\tau} \frac{3.198 \times 10^{-8} T^{1.75}}{p\left(v_i^{\frac{1}{3}} + v_j^{\frac{1}{3}}\right)^2} \left(\sqrt{\frac{1}{M_i} + \frac{1}{M_j}}\right) \quad (19)$$

$$D_{i,k}^{eff} = \frac{\varepsilon}{\tau} \frac{2r_p}{3} \sqrt{\frac{8RT}{\pi M_i}} \quad (20)$$

where $D_{i,j}^{eff}$ and $D_{i,k}^{eff}$ = effective binary diffusion coefficient ($\mathrm{m^2 s^{-1}}$) and Knudsen diffusion coefficient of species i, ($\mathrm{m^2 s^{-1}}$), respectively, ε and τ = porosity and tortuosity, respectively, M_i, M_j = molecular gas, r_p = mean pore radius, p = pressure ($\mathrm{Nm^{-2}}$), and v_i, v_j = diffusion volume.

3.4. Comparative Model Analysis of Ammonia-Fueled H-SOFC with SOFC

Comparative model analysis is also important, along with the solving of mathematical equations to find the more suitable model for ammonia-fueled H-SOFCs. Most of the ammonia-fueled SOFC research work is based on oxygen ion conducting electrolytes, so it is more developed in SOFC modeling than H-SOFC modeling. For O-SOFC modeling, the ANSYS, COMSOL Multiphysics, MATLAB, FORTRAN, PYTHON, etc. programming languages are mainly used for the simulation. But, very few research works based on the ammonia-fueled H-SOFC modeling have been published. Asmare et al. [13] studied the comparative analysis of ammonia-fueled tubular H-SOFCs and O-SOFCs. It is found from many research works that ammonia is fully decomposed for protonic and oxygen ion

conducting SOFCs above 773 K and 1073 K temperatures, respectively [60]. It means that ammonia is completely decomposed for H-SOFCs at intermediate temperatures, but for O-SOFCs, complete ammonia decomposition happens at a higher temperature (1073 K). To understand the ammonia decomposition at different temperatures for different electrolytes, a parametric study is essential, and temperature is incorporated into the cell from 773 K to 1173 K in line with the protonic and oxygen ion temperature limiting condition. The performance of H-SOFCs is higher than O-SOFCs in a similar fuel cell design at low cell temperature, and it is 42 mW/cm^2 and 36 mW/cm^2 for protonic ions and oxygen ions, respectively. At 1073 K or above, the O-SOFC performed better than the H-SOFC, and it was 75 mW/cm^2 and 65 mW/cm^2 for oxygen ions and protonic ions, respectively. Similarly, the polarization and power curve ensure that ammonia-fueled tubular H-SOFCs have a higher concentration and lower ohmic loss than O-SOFCs [13]. Direct ammonia-fueled planar H-SOFCs offer more cost-effective and environmentally friendly benefits than O-SOFCs. They generate a maximum of 147 mW/cm^2 power density at 873K when ammonia is used as fuel on proton-conducting electrolytes [61]. Ni et al. [62] developed a syngas-fueled 2D-H-SOFC model and found that the syngas decreases the H-SOFC performance because carbon-monoxide dilutes the hydrogen concentration. A comparative study for NH_3 and H_2-fueled H-SOFCs [63] showed that ammonia is an outstanding hydrogen carrier and a potential candidate for H-SOFCs because of their hydrogen content and significant cell performance. Kumuk et al. [64] studied the hydrogen and coal gas-fueled 3D-SOFC model for different electrolytes and found that protonic ion solid oxide fuel cells (H-SOFCs) perform better than oxide ion solid oxide fuel cells (O-SOFCs) at medium operating temperatures (400–800 °C) but not at higher temperatures (800–1000 °C).

Mostly, proton conducting materials in the electrolytes shift the location of water production from the anode electrode to the cathode electrode and enable the cell to use the high-energy fuel. The use of numerical modeling in SOFCs can help researchers comprehend multi-physical processes happening inside the cell, experiment with cell performance, and design various elements within a short span of time and in a cost-effective way. To analyze all thermo-physical and electrochemical effects, it is essential to solve the mass, momentum, energy, charge, and species equations simultaneously. In the literature, several researchers have utilized various commercial software packages to simulate SOFCs. Table 4 shows the number of publications where a commercial software package was utilized.

3.5. Research Gap and Future Prospects

In the above discussion, many forms of ammonia-fueled SOFC numerical modeling, including anode-supported, cathode-supported, and electrolyte-supported for various geometrical shapes, take into account the varied temperature profiles. In planar and tubular SOFCs, hydrogen, ammonia, and hydrocarbons are used as fuel to obtain the highest power density at various temperatures. The majority of the experimental and numerical investigations have prioritized anode catalysts for planar SOFCs over tubular SOFCs in order to increase ammonia decomposition. However, very few studies have been conducted on ammonia-fueled tubular SOFCs, particularly those with protonic ion-based hexagonal shapes. We still need to perform more numerical analysis on hexagonal cylindrical H-SOFCs powered by ammonia in contrast to hydrogen and hydrocarbon fuel to produce electricity with no carbon dioxide emissions. In line with the discussion, a few suggestions have been brought up in a few areas that should be taken into consideration in future modeling of the ammonia-fueled H-SOFC.

Table 4. Different types of commercial software packages used in SOFC modeling.

Software Package	Ammonia-Fueled SOFC	Hydrogen-Fueled SOFC	Hydrocarbon-Fueled SOFC	Advantages and Limitations of Software
COMSOL Multiphysics, version 5.3	Anode-supported flat tubular 3D model analysis [10]	Thermal stress analysis on SOFC [65]	Inlet fuel flow analysis in SOFC [66]	COMSOL offers a wide range of benefits, including multiphysics simulation capabilities, a user-friendly interface, flexibility, and customization options. However, it also has limitations related to computational resources, learning curve, cost, model complexity, and post-processing challenges.
	Ammonia usage analysis in the electrolyte-supported SOFC [48]	Ion transition analysis in SOFC [64]	Ion transition analysis in SOFC [64]	
	Analyzing the mechanistic model [67]	Flat tubular SOFC modeling [68]	Flat tubular SOFC modeling [68]	
	Analysis of the flame characteristics for performance improvement of the SOFC model [69]			
	Analysis of the electrochemistry and electrochemical models for SOFC [70]			
MATLAB	Tubular SOFC performance analysis [71]	Tubular SOFC performance analysis [71]	Analysis of the reduced order H-SOFC [72]	MATLAB offers various numerical computing and data visualization capabilities, supported by an extensive library of functions and toolboxes. It has a user-friendly interface and a strong presence in academia and industry. However, it comes with limitations such as cost, performance for certain tasks, memory usage, its closed-source nature, and potential complexities in advanced topics and deployment.
	Analysis of the integration of NH_3-fueled SOFC with gas turbine [73]	Plant-based thermodynamic SOFC modeling analysis [74]	Waste heat and residual fuel composition analysis [75]	
ANSYS	Torsion test, crack installation test, and creep behavior analysis [16]			ANSYS provides a wide range of simulation capabilities, accuracy, physics integration, customization options, and community support. However, it comes with limitations such as cost, learning curve, resource-intensive computations, model complexity, and potential deployment challenges.
FORTRAN	Analysis of the combined hydrogen, heat, and power system in SOFC [76]	Chemical reaction analysis on the SOFC temperature field [77]	Transport and reaction investigations in a 2D SOFC [62]	FORTRAN's strengths lie in numerical performance, legacy code, efficient array operations, and parallel computing. However, it comes with limitations related to syntax complexity, standard libraries, modern language features, and memory management.
Engineering Equation Solver (EES)	One-dimensional H-SOFC analysis [63]	One-dimensional H-SOFC analysis [63]	Integrating SOFC with power and traditional steam [78]	The EES provides valuable capabilities for equation-based engineering problem solving, symbolic manipulation, and parametric studies. Its broad applicability to various engineering fields makes it a useful tool for engineers and scientists. However, it also comes with limitations related to its specific domain, advanced features, customization, and cost considerations.

- Radiative heat transfer analysis is still needed to investigate the ammonia-fueled H-SOFC for temperature-dependent materials, reformations, transportations, and electrochemical reactions.
- One of the major challenges of ammonia-fueled H-SOFC modeling is to maintain low ohmic resistance, separate the higher ohmic overpotential, loss of polarization, and how other parameter affects them.
- Ammonia-fueled anode and cathode concentration overpotential for H-SOFCs is still a dilemma for SOFC research. A more precise dynamic numerical model should be introduced to mitigate the dilemma regarding the anode and cathode concentration of ammonia-fueled H-SOFCs.
- For fuel cell modeling, a fundamental challenge is to obtain the required input data for numerical modeling and validate them with experimental data. Despite the great potential of SOFC modeling, it is still difficult to include all modeling approaches that accurately describe the statistical analysis of fuel cells due to the lack of reliable modeling techniques and data. Today, obtaining data from experimental tests is challenging and sometimes severely constrained, making it more difficult to design fuel cells at an optimal scale. For an optimized fuel cell design, experimental data must be input for comparison with simulated data. This limitation should be removed because it brings difficulties in the fuel cell design analysis.

4. Conclusions

Numerical modeling enables researchers to innovate unique designs and assess the performance of ammonia-fueled H-SOFCs, which leads them to work more in modeling.

Ammonia is brought into the H-SOFC as fuel because it is one the cheapest carbon-free energy sources and stores more energy than hydrocarbon and hydrogen. H-SOFCs are regarded as more suitable for ammonia decomposition due to their low operating temperature, and a low temperature allows SOFCs to operate for a longer time, minimizing the thermal stress and stabilizing the materials. The thermal stress and expansion incongruity between various ceramic components is one of the major issues in SOFC design, and sealing issues also make SOFC fabrication difficult. Therefore, numerical modeling is used to optimize the design and evaluate the performance of ammonia-fueled H-SOFCs. In contrast to experiments, numerical modeling can provide a more realistic scenario of current density, cell voltage, and component concentration as they relate to anode length and time as well as the temperature profile within the cell. Although numerous numerical studies and experimental investigations have been performed on ammonia-fueled H-SOFCs, there are still many untapped potentials in the field of geometrical shapes, cell performance optimization, material development, and ameliorating the lifetime of ammonia-fueled H-SOFCs. Especially at intermediate temperatures, very few significant universal models are available in the literature for analyzing ammonia-fueled H-SOFCs.

Author Contributions: Conceptualization, M.M.R. and A.K.A.; methodology, M.M.R., A.M.A. and A.K.A.; validation, M.M.R. and L.A.O.; formal analysis, M.M.R.; data curation M.M.R., A.K.A. and L.A.O.; writing—original draft preparation, M.M.R.; writing—review and editing, M.M.R., S.A., M.S.R., M.R.S. and A.K.A.; visualization, V.R. and S.A.; supervision, M.R.S., V.R. and A.K.A. All authors have read and agreed to the published version of the manuscript.

Funding: This research received no external funding.

Data Availability Statement: Not applicable.

Acknowledgments: The authors M.M.R. and L.A.O. acknowledge the support from Universiti Brunei Darussalam through the University Graduate Scholarship.

Conflicts of Interest: The authors declare no conflict of interest.

References

1. Hajimolana, S.A.; Hussain, M.A.; Daud, W.M.A.W.; Soroush, M.; Shamiri, A. Mathematical modeling of solid oxide fuel cells: A review. *Renew. Sustain. Energy Rev.* **2011**, *15*, 1893–1917. [CrossRef]
2. Wang, B.; Li, T.; Gong, F.; Othman, M.H.D.; Xiao, R. Ammonia as a green energy carrier: Electrochemical synthesis and direct ammonia fuel cell—A comprehensive review. *Fuel Process. Technol.* **2022**, *235*, 107380. [CrossRef]
3. Zainon, A.N.; Somalu, M.R.; Bahrain, A.M.K.; Muchtar, A.; Baharuddin, N.A.; SA, M.A.; Osman, N.; Samat, A.A.; Azad, A.K.; Brandon, N.P. Challenges in using perovskite-based anode materials for solid oxide fuel cells with various fuels: A review. *Int. J. Hydrogen Energy* **2023**, *48*, 20441–20464. [CrossRef]
4. Azad, A.K.; Abdalla, A.M.; Afif, A.; Azad, A.; Afroze, S.; Idris, A.C.; Park, J.-Y.; Saqib, M.; Radenahmad, N.; Hossain, S.; et al. Improved mechanical strength, proton conductivity and power density in an 'all-protonic' ceramic fuel cell at intermediate temperature. *Sci. Rep.* **2021**, *11*, 19382. [CrossRef]
5. Lee, T.H.; Park, K.Y.; Kim, N.I.; Song, S.J.; Hong, K.H.; Ahn, D.; Azad, A.K.; Hwang, J.; Bhattacharjee, S.; Lee, S.C.; et al. Robust $NdBa_{0.5}Sr_{0.5}Co_{1.5}Fe_{0.5}O_{5+\delta}$ cathode material and its degradation prevention operating logic for intermediate temperature-solid oxide fuel cells. *J. Power Sources* **2016**, *331*, 495–506. [CrossRef]
6. Abdalla, A.M.; Hossain, S.; Nisfindy, O.B.; Azad, A.T.; Dawood, M.; Azad, A.K. Hydrogen production, storage, transportation and key challenges with applications: A review. *Energy Convers. Manag.* **2018**, *165*, 602–627. [CrossRef]
7. Radenahmad, N.; Azad, A.T.; Saghir, M.; Taweekun, J.; Bakar, M.S.A.; Reza, M.S.; Azad, A.K. A review on biomass derived syngas for SOFC based combined heat and power application. *Renew. Sustain. Energy Rev.* **2020**, *119*, 109560. [CrossRef]
8. Afif, A.; Radenahmad, N.; Cheok, Q.; Shams, S.; Kim, J.H.; Azad, A.K. Ammonia-fed fuel cells: A comprehensive review. *Renew. Sustain. Energy Rev.* **2016**, *60*, 822–835. [CrossRef]
9. Valera-Medina, A.; Amer-Hatem, F.; Azad, A.K.; Dedoussi, I.C.; de Joannon, M.; Fernandes, R.X.; Glarborg, P.; Hashemi, H.; He, X.; Mashruk, S.; et al. Review on Ammonia as a Potential Fuel: From Synthesis to Economics. *Energy Fuels* **2021**, *35*, 6964–7029. [CrossRef]
10. Ilbas, M.; Alemu, M.A.; Cimen, F.M. Comparative performance analysis of a direct ammonia-fuelled anode supported flat tubular solid oxide fuel cell: A 3D numerical study. *Int. J. Hydrogen Energy* **2022**, *47*, 3416–3428. [CrossRef]

11. Oh, S.; Oh, M.J.; Hong, J.; Yoon, K.J.; Ji, H.-I.; Lee, J.-H.; Kang, H.; Son, J.-W.; Yang, S. A comprehensive investigation of direct ammonia-fueled thin-film solid-oxide fuel cells: Performance, limitation, and prospects. *iScience* **2022**, *25*, 105009. [CrossRef] [PubMed]
12. Asmare, M.; Ilbas, M.; Cimen, F.M.; Timurkutluk, C.; Onbilgin, S. Three-dimensional numerical simulation and experimental validation on ammonia and hydrogen fueled micro tubular solid oxide fuel cell performance. *Int. J. Hydrogen Energy* **2022**, *47*, 15865–15874. [CrossRef]
13. Asmare, M.; Ilbas, M.; Yalcin, S. Numerical modelling and comparative analysis of direct ammonia fuelled protonic and oxygen-ion conducting tubular solid oxide fuel cell. *Int. J. Hydrogen Energy* **2021**, *46*, 36878–36889. [CrossRef]
14. Radenahmad, N.; Afif, A.; Petra, P.I.; Rahman, S.M.H.; Eriksson, S.-G.; Azad, A.K. Proton-conducting electrolytes for direct methanol and direct urea fuel cells—A state-of-the-art review. *Renew. Sustain. Energy Rev.* **2016**, *57*, 1347–1358. [CrossRef]
15. Hossain, S.; Abdalla, A.M.; Suhaili, S.B.H.; Kamal, I.; Shaikh, S.P.S.; Dawood, M.K.; Azad, A.K. Nanostructured graphene materials utilization in fuel cells and batteries: A review. *J. Energy Storage* **2020**, *29*, 101386. [CrossRef]
16. Dhanasekaran, A.; Subramanian, Y.; Omeiza, L.A.; Raj, V.; Yassin, H.P.H.M.; SA, M.A.; Azad, A.K. Computational Fluid Dynamics for Protonic Ceramic Fuel Cell Stack Modeling: A Brief Review. *Energies* **2022**, *16*, 208. [CrossRef]
17. Hossain, S.; Abdalla, A.M.; Zaini, J.H.; Savaniu, C.D.; Irvine, J.T.S.; Azad, A.K. Highly dense and novel proton conducting materials for SOFC electrolyte. *Int. J. Hydrogen Energy* **2017**, *42*, 27308–27322. [CrossRef]
18. Hossain, S.; Abdalla, A.M.; Jamain, S.N.B.; Zaini, J.H.; Azad, A.K. A review on proton conducting electrolytes for clean energy and intermediate temperature-solid oxide fuel cells. *Renew. Sustain. Energy Rev.* **2017**, *79*, 750–764. [CrossRef]
19. Afroze, S.; Karim, A.; Cheok, Q.; Eriksson, S.; Azad, A.K. Latest development of double perovskite electrode materials for solid oxide fuel cells: A review. *Front. Energy* **2019**, *13*, 770–797. [CrossRef]
20. Hussain, S.; Li, Y. Review of solid oxide fuel cell materials: Cathode, anode, and electrolyte. *Energy Transit.* **2020**, *4*, 113–126. [CrossRef]
21. Fergus, J.W. Electrolytes for solid oxide fuel cells. *J. Power Sources* **2006**, *162*, 30–40. [CrossRef]
22. Dalslet, B.; Blennow, P.; Hendriksen, P.V.; Bonanos, N.; Lybye, D.; Mogensen, M. Assessment of doped ceria as electrolyte. *J. Solid State Electrochem.* **2006**, *10*, 547–561. [CrossRef]
23. Shi, H.; Su, C.; Ran, R.; Cao, J.; Shao, Z. Electrolyte materials for intermediate-temperature solid oxide fuel cells. *Prog. Nat. Sci. Mater. Int.* **2020**, *30*, 764–774. [CrossRef]
24. Biswas, S.; Kaur, G.; Paul, G.; Giddey, S. A critical review on cathode materials for steam electrolysis in solid oxide electrolysis. *Int. J. Hydrogen Energy.* **2023**, *48*, 12541–12570. [CrossRef]
25. Xu, H.; Dang, L.; Yan, J.; Wan, F.; Gong, W. Preparation of a nano-size $(La_{0.2}Nd_{0.2}Sm_{0.2}Sr_{0.2}Ba_{0.2})Co_{0.2}Fe_{0.8}O_{3-\delta}$/SDC high-entropy oxide composite cathode. *Mater. Lett.* **2023**, *338*, 134029. [CrossRef]
26. Azad, A.K.; Irvine, J.T.S. Synthesis, chemical stability and proton conductivity of the perovksites $Ba(Ce,Zr)_{1-x}\ Sc_x\ O_{3-\delta}$. *Solid State Ion* **2007**, *178*, 635–640. [CrossRef]
27. Radenahmad, N.; Afif, A.; Petra, M.I.; Rahman, S.M.H.; Eriksson, S.; Azad, A.K. High conductivity and high density proton conducting $Ba_{1-x}Sr_xCe_{0.5}Zr_{0.35}Y_{0.1}Sm_{0.05}O_{3-\delta}$(x = 0.5, 0.7, 0.9, 1.0) perovskites for IT-SOFC. *Int. J. Hydrogen Energy* **2016**, *41*, 11832–11841. [CrossRef]
28. Afif, A.; Radenahmad, N.; Lim, C.M.; Petra, M.I.; Islam, M.A.; Rahman, S.M.H.; Eriksson, S.; Azad, A.K. Structural study and proton conductivity in $BaCe_{0.7}Zr_{0.25-x}Y_xZn_{0.05}O_3$(x = 0.05, 0.1, 0.15, 0.2 & 0.25). *Int. J. Hydrogen Energy* **2016**, *41*, 11823–11831. [CrossRef]
29. Rathore, S.S.; Biswas, S.; Fini, D.; Kulkarni, A.P.; Giddey, S. Direct ammonia solid-oxide fuel cells: A review of progress and prospects. *Int. J. Hydrogen Energy* **2021**, *46*, 35365–35384. [CrossRef]
30. Kaur, P.; Singh, K. Review of perovskite-structure related cathode materials for solid oxide fuel cells. *Ceram. Int.* **2020**, *46*, 5521–5535. [CrossRef]
31. Aziz, A.J.A.; Baharuddin, N.A.; Somalu, M.R.; Muchtar, A. Review of composite cathodes for intermediate-temperature solid oxide fuel cell applications. *Ceram. Int.* **2020**, *46*, 23314–23325. [CrossRef]
32. Gao, Y.; Huang, X.; Yuan, M.; Gao, J.; Wang, Z.; Abdalla, A.M.; Azad, A.K.; Xu, L.; Lv, Z.; Wei, B. A SrCo0.9Ta0.1O3-δ derived medium-entropy cathode with superior CO_2 poisoning tolerance for solid oxide fuel cells. *J. Power Sources* **2022**, *540*, 231661. [CrossRef]
33. Cowin, P.I.; Petit, C.T.G.; Lan, R.; Irvine, J.T.S.; Tao, S. Recent Progress in the Development of Anode Materials for Solid Oxide Fuel Cells. *Adv. Energy Mater.* **2011**, *1*, 314–332. [CrossRef]
34. Hua, B.; Yan, N.; Li, M.; Sun, Y.F.; Zhang, Y.Q.; Li, J.; Etsell, T.; Sarkar, P.; Luo, J.L. Anode-Engineered Protonic Ceramic Fuel Cell with Excellent Performance and Fuel Compatibility. *Adv. Mater.* **2016**, *28*, 8922–8926. [CrossRef] [PubMed]
35. Boukamp, B.A. Fuel cells: The amazing perovskite anode. *Nat. Mater.* **2003**, *2*, 294–296. [CrossRef]
36. Prakash, B.S.; Kumar, S.S.; Aruna, S.T. Properties and development of Ni/YSZ as an anode material in solid oxide fuel cell: A review. *Renew. Sustain. Energy Rev.* **2014**, *36*, 149–179. [CrossRef]
37. Pihlatie, M.; Kaiser, A. Mogensen, Redox stability of SOFC: Thermal analysis of Ni–YSZ composites. *Solid State Ion.* **2009**, *180*, 1100–1112. [CrossRef]

38. Boldrin, P.; Ruiz-Trejo, E.; Mermelstein, J.; Menéndez, J.M.B.; Ramı, T.; Brandon, N.P. Strategies for Carbon and Sulfur Tolerant Solid Oxide Fuel Cell Materials, Incorporating Lessons from Heterogeneous Catalysis. *Chem. Rev.* **2016**, *116*, 13633–13684. [CrossRef]
39. Rafique, M.; Nawaz, H.; Rafique, M.S.; Tahir, M.B.; Nabi, G.; Khalid, N.R. Material and method selection for efficient solid oxide fuel cell anode: Recent advancements and reviews. *Int. J. Energy Res.* **2019**, *43*, 2423–2446. [CrossRef]
40. Tao, S.; Irvine, J.T.S. A redox-stable efficient anode for solid-oxide fuel cells. *Nat. Mater.* **2003**, *2*, 320–323. [CrossRef]
41. Ghosh, A.; Azad, A.; Irvine, J.T. Study of Ga Doped LSCM as an Anode for SOFC. *ECS Trans.* **2011**, *35*, 1337–1343. [CrossRef]
42. Yang, J.; Akagi, T.; Okanishi, T.; Muroyama, H.; Matsui, T.; Eguchi, K. Catalytic Influence of Oxide Component in Ni-Based Cermet Anodes for Ammonia-Fueled Solid Oxide Fuel Cells. *Fuel Cells* **2015**, *15*, 390–397. [CrossRef]
43. Ni, M.; Leung, M.K.H.; Leung, D.Y.C. Ammonia-fed solid oxide fuel cells for power generation-A review. *Int. J. Energy Res.* **2009**, *33*, 943–959. [CrossRef]
44. Ghorbani, B.; Vijayaraghavan, K. A review study on software-based modeling of hydrogen-fueled solid oxide fuel cells. *Int. J. Hydrogen Energy* **2019**, *44*, 13700–13727. [CrossRef]
45. Faheem, H.H.; Abbas, S.Z.; Tabish, A.N.; Fan, L.; Maqbool, F. A review on mathematical modelling of Direct Internal Reforming-Solid Oxide Fuel Cells. *J. Power Sources* **2022**, *520*, 230857. [CrossRef]
46. Ni, M. Thermo-electrochemical modeling of ammonia-fueled solid oxide fuel cells considering ammonia thermal decomposition in the anode. *Int. J. Hydrogen Energy* **2011**, *36*, 3153–3166. [CrossRef]
47. Wojcik, A.; Middleton, H.; Damopoulos, I.; Van Herle, J. Ammonia as a fuel in solid oxide fuel cells. *J. Power Sources* **2003**, *118*, 342–348. [CrossRef]
48. Ilbas, M.; Kumuk, B.; Alemu, M.A.; Arslan, B. Numerical investigation of a direct ammonia tubular solid oxide fuel cell in comparison with hydrogen. *Int. J. Hydrogen Energy* **2020**, *45*, 35108–35117. [CrossRef]
49. Gould, H.; Tobochnik, J.; Christian, W. An Introduction to Computer Simulation Methods: Applications to Physical Systems (third edition). *Am. J. Phys.* **2006**, *74*, 652–653. [CrossRef]
50. Chen, Y.; Qin, W. A variable range step technique for propagation predictions over large irregular terrain using the Fourier split-step parabolic equation. In Proceedings of the 2015 Asia-Pacific Microwave Conference (APMC), Nanjing, China, 6–9 December 2015; Volume 2, pp. 1–3. [CrossRef]
51. Li, C.Z.; Wang, S. The finite volume method and application in combinations. *J. Comput. Appl. Math.* **1999**, *106*, 21–53. [CrossRef]
52. Yahya, A.; Naji, H.; Dhahri, H. A lattice Boltzmann analysis of the performance and mass transport of a solid oxide fuel cell with a partially obstructed anode flow channel. *Fuel* **2023**, *334*, 126537. [CrossRef]
53. Adami, S.; Hu, Y.X.; Adams, A.N. A generalized wall boundary condition for smoothed particle hydrodynamics. *J. Comput. Phys.* **2012**, *231*, 7057–7075. [CrossRef]
54. Fahmy, A.M. A new boundary element algorithm for modeling and simulation of nonlinear thermal stresses in micropolar FGA composites with temperature-dependent properties. *Adv. Model. Simul. Eng. Sci* **2021**, *8*, 6. [CrossRef]
55. Pazirofteh, M.; Dehghani, M.; Niazi, S.; Mohammadi, H.A.; Asghari, M. Molecular dynamics simulation and Monte Carlo study of transport and structural properties of PEBA 1657 and 2533 membranes modified by functionalized POSS-PEG material. *J. Mol. Liq.* **2017**, *241*, 646–653. [CrossRef]
56. Yu, P.; Ren, Z.; Chen, Z.; Bordas, A.P.S. A multiscale finite element model for prediction of tensile strength of concrete. *Finite Elem. Anal. Des.* **2023**, *215*, 103877. [CrossRef]
57. Gooneie, A.; Schuschnigg, S.; Holzer, C. A Review of Multiscale Computational Methods in Polymeric Materials. *Polymers* **2017**, *9*, 16. [CrossRef]
58. Ezzat, M.F.; Dincer, I. Energy and exergy analyses of a novel ammonia combined power plant operating with gas turbine and solid oxide fuel cell systems. *Energy* **2020**, *194*, 116750. [CrossRef]
59. Osman, N.; Mazlan, N.A.; Affandi, N.S.M.; Mazlan, N.W.; Jani, A.M.M. Optimization of electrolyte performance by tailoring the structure and morphology of Ba(Ce,Zr)O_3 ceramics with different types of surfactants. *Ceram. Int.* **2020**, *46*, 27401–27409. [CrossRef]
60. Ni, M.; Leung, D.; Leung, M. Mathematical modeling of ammonia-fed solid oxide fuel cells with different electrolytes. *Int. J. Hydrogen Energy* **2008**, *33*, 5765–5772. [CrossRef]
61. Zhang, L.; Yang, W. Direct ammonia solid oxide fuel cell based on thin proton-conducting electrolyte. *J. Power Sources* **2008**, *179*, 92–95. [CrossRef]
62. Ni, M.; Shao, Z.; Chan, K. Modeling of Proton-Conducting Solid Oxide Fuel Cells Fueled with Syngas. *Energies* **2014**, *7*, 4381–4396. [CrossRef]
63. Kalinci, Y.; Dincer, I. Analysis and performance assessment of NH_3 and H_2 fed SOFC with proton-conducting electrolyte. *Int. J. Hydrogen Energy* **2018**, *43*, 5795–5807. [CrossRef]
64. Kumuk, B.; Alemu, M.A.; Ilbas, M. Investigation of the effect of ion transition type on performance in solid oxide fuel cells fueled hydrogen and coal gas. *Int. J. Hydrogen Energy* **2022**, *47*, 3409–3415. [CrossRef]
65. Cai, W.; Yuan, J.; Zheng, Q.; Yu, W.; Yin, Z.; Zhang, Z.; Pei, Y.; Li, S. Numerical Investigation of Heat/Flow Transfer and Thermal Stress in an Anode-Supported Planar SOFC. *Crystals* **2022**, *12*, 1697. [CrossRef]
66. Kümük, B.; İlbaş, M. Coal gas fuel utilization effects on electrolyte supported solide oxide fuel cell performance. *Int. J. Hydrogen Energy* **2021**, *46*, 29523–29528. [CrossRef]

67. Luo, Y.; Shi, Y.; Liao, S.; Chen, C.; Zhan, Y.; Au, C.-T.; Jiang, L. Coupling ammonia catalytic decomposition and electrochemical oxidation for solid oxide fuel cells: A model based on elementary reaction kinetics. *J. Power Sources* **2019**, *423*, 125–136. [CrossRef]
68. Cimen, F.M.; Kumuk, B.; Ilbas, M. Simulation of hydrogen and coal gas fueled flat-tubular solid oxide fuel cell (FT-SOFC). *Int. J. Hydrogen Energy* **2022**, *47*, 3429–3436. [CrossRef]
69. Ilbas, M.; Karyeyen, S.; Cimen, F.M. Numerical investigation of combustion and flame characteristics for a model solid oxide fuel cell performance improvement. *Fuel* **2022**, *322*, 124188. [CrossRef]
70. Zhang, X.; Wang, L.; Espinoza, M.; Li, T.; Andersson, M. Numerical simulation of solid oxide fuel cells comparing different electrochemical kinetics. *Int. J. Energy Res.* **2021**, *45*, 12980–12995. [CrossRef]
71. Hajimolana, S.A.; Hussain, M.A.; WanDaud, W.M.A. Comparative study on the performance of a tubular solid oxide fuel cell fuelled by ammonia and hydrogen. In Proceedings of the CHEMECA Annual Conference 2011, Sydney, Australia, 18–21 September 2011.
72. Milewski, J.; Szczęśniak, A.; Szabłowski, Ł. A proton conducting solid oxide fuel cell—Implementation of the reduced order model in available software and verification based on experimental data. *J. Power Sources* **2021**, *502*, 229948. [CrossRef]
73. Ishak, F.; Dincer, I.; Zamfirescu, C. Energy and exergy analyses of direct ammonia solid oxide fuel cell integrated with gas turbine power cycle. *J. Power Sources* **2012**, *212*, 73–85. [CrossRef]
74. Alsarraf, J.; Alnaqi, A.A.; Al-Rashed, A.A.A.A. Thermodynamic modeling and exergy investigation of a hydrogen-based integrated system consisting of SOFC and CO_2 capture option. *Int. J. Hydrogen Energy* **2022**, *47*, 26654–26664. [CrossRef]
75. Huang, Y.; Lin, Q.; Liu, H.; Ni, M.; Zhang, X. Evaluation of the waste heat and residual fuel from the solid oxide fuel cell and system power optimization. *Int. J. Heat Mass Transf.* **2017**, *115*, 1166–1173. [CrossRef]
76. Perna, A.; Minutillo, M.; Jannelli, E.; Cigolotti, V.; Nam, S.W.; Han, J. Design and performance assessment of a combined heat, hydrogen and power (CHHP) system based on ammonia-fueled SOFC. *Appl. Energy* **2018**, *231*, 1216–1229. [CrossRef]
77. Zitouni, B.; Andreadis, G.M.; Hocine, B.M.; Hafsia, A.; Djamel, H.; Mostefa, Z. Two-dimensional numerical study of temperature field in an anode supported planar SOFC: Effect of the chemical reaction. *Int. J. Hydrogen Energy* **2011**, *36*, 4228–4235. [CrossRef]
78. Al-Khori, K.; Bicer, Y.; Boulfrad, S.; Koç, M. Techno-economic and environmental assessment of integrating SOFC with a conventional steam and power system in a natural gas processing plant. *Int. J. Hydrogen Energy* **2019**, *44*, 29604–29617. [CrossRef]